COMBINING THE NON-LINEARITY OF ANGLE-PLIES AND FIBRE FRAGMENTATION IN CARBON FIBRE LAMINATES UNDER COMPRESSIVE LOADING

X. Wu*, J.D. Fuller and M.R. Wisnom

Bristol Composites Institute (ACCIS), University of Bristol, Bristol, UK, BS8 1TR
*Email: Xunxun.Wu@bristol.ac.uk, web page: http://hiperduct.ac.uk/

Keywords: Pseudo-ductility, thin plies, angle-ply, compression, mechanical testing

ABSTRACT

The aim of this work is to experimentally explore the potential of using the thin ply angle-ply concept for achieving compressive pseudo-ductility in carbon fibre laminates. A laminate with a $[\pm 27_7/0]_s$ configuration was selected and tested in compression, via a sandwich beam subjected to four-point bending. From the moment versus strain curve, a significant amount of non-linearity has been observed and an average failure strain of 1.08% has been attained. Visual damage observation of a single fracture parallel to the angle-ply direction and the high shear stress suggest that the compressive failure can be attributed to the low ply shear strength.

1 INTRODUCTION

Pseudo-ductile carbon fibre reinforced plastic (CFRP) laminates have been developed via different approaches within the High Performance Ductile Composites Technologies (HiPerDucT) programme in order to overcome brittle failure and to achieve a gradual failure in carbon fibre laminates [1–4]. For example, a metal-like stress-strain tensile behaviour was obtained in a thin ply angle-ply laminate $[\pm\theta_m/0_n]_s$ by Fuller and Wisnom. This approach is based on combining the fibre re-orientation with gradual fibre fragmentation in the central 0° plies [3].

Up to now, work has focused primarily on tensile loading. To be able to extend the pseudo-ductile thin ply angle-ply laminates to more applications, compressive performance is a key design consideration as it is usually much lower than the tensile performance. In conventional uni-directional (UD) carbon fibre laminates, the main compressive failure mode is plastic microbuckling or kinking [5]. Previous studies have indicated that in the case of off-axis laminates with internal UD plies $[\pm\theta_m/0_2]_s$ subjected to compressive loading, laminates failed catastrophically after delamination initiated from the kink-band, leading to the internal UD plies being unsupported by the angle-plies [5].

Lee and Soutis conducted several studies on the scaling and thickness effect on compressive behaviour of carbon fibre laminates [6]. Sublaminate-level and ply-level scaled quasi-isotropic (QI) specimens with different ply thicknesses of 0.125mm and 0.25mm were tested in compression. The results revealed that with an increase in ply thickness or number of blocked plies, the compressive strength reduced significantly and the number of delaminations and matrix cracks increased. It was also noted that the failure modes of the laminate changed from microbuckling in the 0° plies to delamination dominated failure when the thickness of blocked plies increased from 0.25mm to 1mm.

Similar observations have been seen in thin ply laminates. Arteiro et al. found that in compression, the thin ply laminate failed in a brittle, net-section manner, dominated by fibre kinking [7]. They also found that the laminate with a ply "blocking" layup showed an increase in delamination initiated after fibre-kinking, with strength significantly lower compared with a laminate with a standard ply thickness (t = 0.125mm). Amacher et al. tested UD laminates in compression with three different ply thicknesses, and the results showed the trend that the compressive strength increased with decreasing ply thickness [8]. By using optical microscopy, more uniform microstructures, with better fibre

alignment and a smaller resin rich region were observed in the thinnest plies, which resulted in a better compressive performance in thin ply laminates.

The aim of this work is to experimentally explore the potential of using the thin ply angle-ply concept for achieving compressive pseudo-ductility in a carbon fibre laminate, since the research above has shown that if the ply is sufficiently thin, delamination can be suppressed in compressive loading [7,8]. In this paper, laminates were designed with a $[\pm 27_7/0]_s$ layup and tested under an indirect compressive loading using a sandwich beam in bending.

2 EXPERIMENTS

2.1 Compression test methods selection:

A number of test methods are available to determine the compressive behaviour of carbon fibre laminates, either direct compression tests (ASTM D695 [9] and ASTM D3410 [10]) or indirect compression tests (ASTM D5467 [11] and the hybrid beam bending test [1]). Different testing methods can bring significant discrepancies in results, therefore the selection of a test method needs to be well considered. In this paper, an indirect compression testing method via a 4-point bend of a sandwich beam was selected. Several considerations in choosing this method were made here. First of all, the direct test methods via end-loading require a high precision in specimen machining and can easily result in failure in undesired failure modes, such as failure in the end-tab due to the stress-concentration. The second consideration is made from material usage efficiency. Due to the low ply thickness (t=0.03mm), to satisfy the thickness requirement for direct testing requires a large number of plies, which is not ideal. Thirdly, a specimen gauge length of 10 mm is usually used in direct compression, which is not ideal for angle-ply testing, since the fibre rotation is limited by the end-tabs. In addition, due to the large fibre rotation of angle plies and the Poisson ratio effects, the hybrid beam bending method [1] is not suited for this case, due to the mismatch of the Poisson ratio of the angle-ply laminate and glass substrate.

2.2 Specimen sizing and beam sizing:

Progressive fibre fractures of M55 high modulus carbon fibre in compression were observed in a glass-carbon hybrid beam under the four-point bending loading presented by Czel and Wisnom [1]. In order to promote the gradual fragmentation in the central 0° plies instead of a single-fracture of the laminate, the stress concentration at the crack tip needs to be taken into consideration:

$$\sigma_{crack} = K_t \sigma_x \left(\frac{t}{t_{AP}} \right) \tag{1}$$

Where K_t is a stress concentration factor of 1.08 in this case, σ_x is the laminate applied stress, t_{AP} is the thickness of angle plies and t is the total laminate thickness [3]. A $[\pm 27_7/0]_s$ combination was tested, since ±27° is expected to show the promising combination of nonlinearity and considerable strength.

The material used for the angle plies was the Skyflex UIN020 prepreg with Mitsubishi Rayon MR60 intermediate modulus fibre (denoted as IM) and for the 0° plies was the North M55JB-ThinPreg120EPHTg-402 prepreg with M55 high modulus fibre (denoted as HM). The Skyflex prepreg uses K50 semi-toughened low-temperature cure resin and the North prepreg uses a 120EPHTg-402 type epoxy resin system. The elastic properties of the cured prepregs are given in Table 1.

Table 1: Cured ply properties of UD laminates

		Skyflex UIN020A	M55/Epoxy[1]	IM7/8552 [12]
E_1	[GPa]	146	280	164
E_2	[GPa]	6.6	6.2	11.4
σ_l	[MPa]	2800	2240	2723
G_{12}	[GPa]	2.97	5.0	5.17
ε_{1c}	[%]	-	0.456	-
t	[mm]	0.028	0.032	0.125
V_f	[%]	50	50	60

Nomex-3.2-144 honeycomb with a height of 13.75mm has been selected as the sandwich core. The compressive modulus and the shear strength in the ribbon direction are 0.6 GPa and 128MPa respectively [13]. The ASTM standard [11] recommends that the thickness of the bottom skin should be at least twice that of the top skin to avoid failure in the tensile side. Large amounts of materials would be required if using the same thin ply prepreg in the bottom skin. As an alternative, the standard thickness prepreg Hexcel IM7/8552 with a layup $[\pm 27_3/0]_s$ was selected for the bottom skin. Once the materials and layup were determined, the next step was to design the test beam carefully to promote compressive failure in the top skin without premature failure in the core, due to shear for example [14]. The sizing results of the test sandwich beam are illustrated in Figure 1 and presented in Table 2.

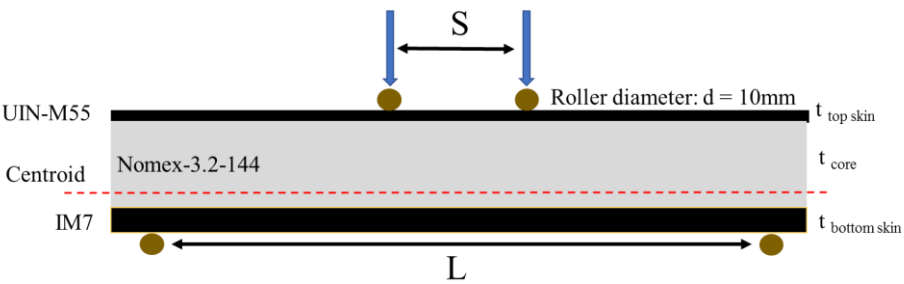

Figure 1: Specimen schematic for test sandwich beam and test setup geometry

Table 2: Sizing results for test sandwich beam

Sizing results		$[\pm 27_7/0]_s$
L	[mm]	340
S	[mm]	40
Width	[mm]	30
$t_{top\ skin}$	[mm]	0.75
$t_{bottom\ skim}$	[mm]	1.75
t_{total}	[mm]	16.60

2.3 Manufacture and testing:

The sandwich beam was manufactured using a post-cure bonding method. Firstly, the top and bottom skins were cured separately in the autoclave using their specific curing cycles. Then both skins were bonded to the honeycomb core with a FM 73M epoxy adhesive film between each of the components and the entire assembled structure was cured in the oven at 120°C, following the specified cure cycle [15]. The bonded panel was machined to the required dimensions as shown previously.

Five specimens were tested in total using a four-point bending test fixture, with loading and support roller diameters of 10mm. Two strain gauges were placed on the surface of the top and bottom skins to measure longitudinal strains, and another strain gauge was placed perpendicularly on the surface of the top skin to measure transverse strain. All tests were performed using an Instron 25kN hydraulically-actuated testing machine with a loading rate of 2mm/min. The test configuration is shown in Figure 2.

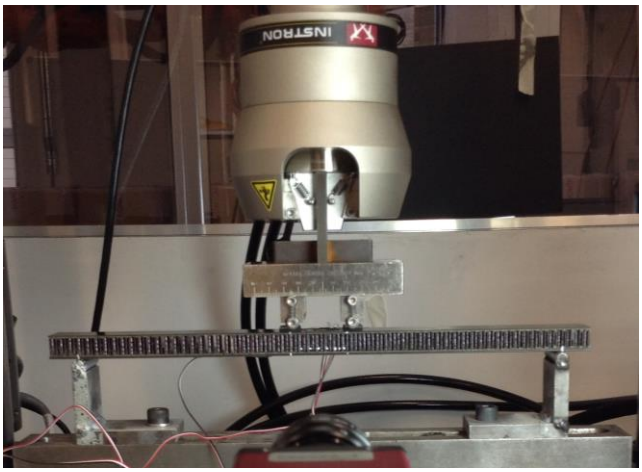

Figure 2: Illustration of the test setup

3 RESULTS AND DISCUSSION

As expected, all five specimens failed in the compressive skin and no undesirable failure modes, such as core shear failure, occurred. Since the deflection of the beam is small, the applied moment calculated from the applied load times a constant moment arm, and the applied moment per unit width was plotted versus the surface strains for the test beam under bending in Figure 3. The longitudinal compressive strain ε_{tx} increased linearly with the applied moment in the initial stage. When the strain reached a compressive strain of 5600 $\mu\varepsilon$, the slope of the moment-strain curve reduced significantly. At this point, the fracture strain of the M55 fibre had been reached and the central 0° plies fractured progressively. This process is slightly different to the stress plateau presented for the pseudo-ductile thin ply angle-ply specimen loaded in tension, which has shown an approximately constant stress level during the fibre fragmentation. Also, it is noted that significant non-linearity developed in the transverse direction of the compressive skin and the transverse strain was almost twice that of the longitudinal strain. The moment-strain curve of the lower tensile skin showed a fairly linear behaviour as it was operating at a low strain range.

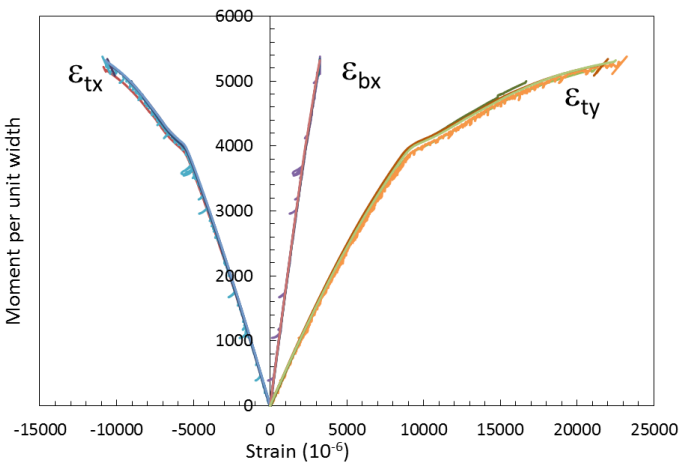

Figure 3: Applied moment per unit width versus surface strains of test beam under four-point bending

From visual inspection as presented in Figure 4, the specimen failed in a single-fracture through the thickness and across the entire width of the compressive skin, parallel to the –27° direction. This has been shown as a common failure mode in angle-ply laminates in compression. The high shear stress in the angle-ply laminates in compression, resulted in a reduction in the compressive strength [16,17]. The failure modes in this case include matrix failure in the -27° plies, fibre fracture in the 27° plies and possible fragmentation in the central 0° plies. Due to delamination at the 0/-θ interface being inhibited, the laminate did not fail immediately after the central 0° plies fragmented and the angle plies took up further loading until final failure.

From Figure 4, it also can be seen that the fracture developed from one end near the loading roller to the other end outside of the loading span. Some localised core damage was seen in the red-box, but this happened after compressive failure of the skin and there was no load drop prior to final failure, as can be observed in Figure 3. The core damage was crushing due to the large amount of energy that was released in the compressive fracture in the skin.

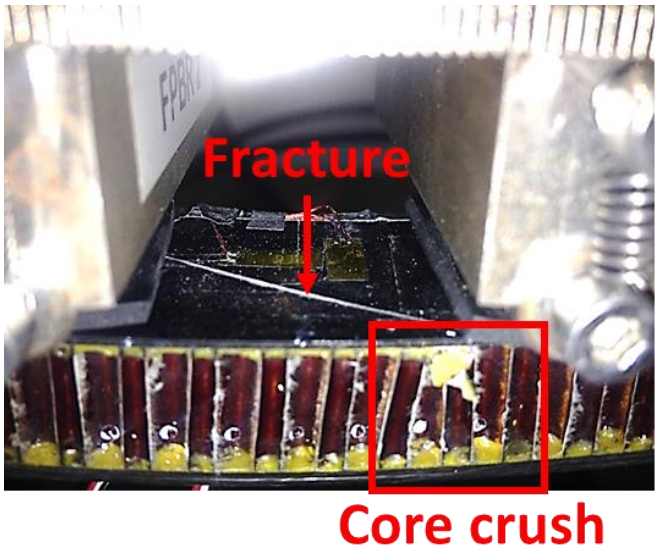

Figure 4: Failure mode exhibited in the sandwich beam

To understand the low strain to failure and ply-level behaviour further, ply level stresses and strains were calculated using Classical Laminate Theory (CLT) from the experimental surface strains measurements, with constant material properties from Table 1 and ignoring fibre rotation and fibre fragmentation. The results of σ_{11}-ε_{11}, σ_{22}-ε_{22} and τ_{12}-γ_{12} are plotted in Figure 5.

As seen from the stress-strain curves, the stress level in the fibre direction σ_{11} was the greatest. However, comparing those values with the material properties presented in Table 3, it can be seen that the ply level stresses of τ_{12} and σ_{22} were very high. The calculated shear stress τ_{12} was higher than the material in-plane shear yield strength of 50 MPa, and the stress developed in the transverse direction σ_{22} was also close to the ultimate transverse strength of the Skyflex UIN020 prepreg. This obervation suggested that the low stress at failure of the angle-ply laminates under compressive loading could mainly be attributed to the high in-plane shear and transverse stresses.

Table 3: Material direction stress and strain calculated from CLT

		From CLT	Material properties[18]
σ_{11}	[MPa]	-518	-1440
σ_{22}	[MPa]	75	82
τ_{12}	[MPa]	56	50
ε_{11}	[με]	-3800	N/A
ε_{22}	[με]	15600	N/A
γ_{12}	[με]	26700	N/A

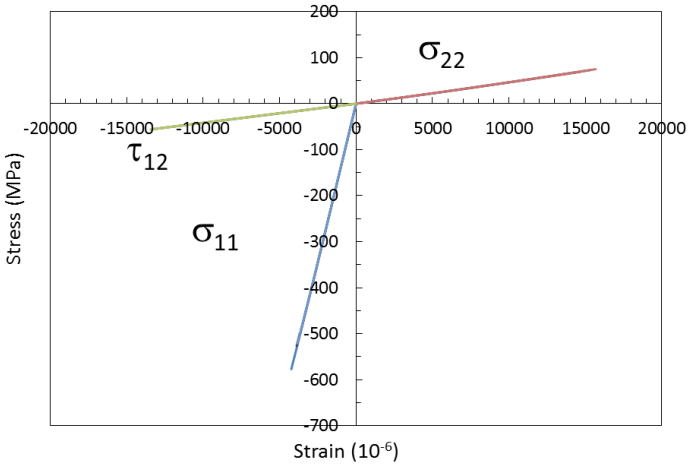

Figure 5: Material direction stress-strain plot calculated from CLT

4 CONCLUSIONS

In this study, a thin ply angle-ply laminate with internal 0° plies has been experimentally tested via an indirect compressive test method using a sandwich beam. The laminate exhibited a non-linear compressive moment-strain curve and the curve mainly consisted of an initial elastic region, fibre fragmentation in the central 0° plies, and a section of further loading of the angle plies. The failure mode of the specimen was a single fracture, parallel to the -27° direction due to high shear stress within the angle-ply laminate in compression. It also has been shown that delaminations were suppressed in the thin ply laminate and multiple fibre fractures were promoted, instead of a single complete delamination initiated from the fibre fracture surface.

ACKNOWLEDGEMENTS

This work was funded by the ACCIS Centre for Doctoral Training in Advanced Composites (grant number EP/G036772/1) and under the UK Engineering and Physical Sciences Research Council (EPSRC) Programme Grant EP/I02946X/1 on High Performance Ductile Composite Technology in collaboration with Imperial College, London.

REFERENCES

[1] Czel G, Jalalvand M, Wisnom MR. Hybrid specimens eliminating stress concentrations in tensile and compressive testing of unidirectional composites. Compos Part A Appl Sci Manuf 2016;91:436–47.

[2] Czél G, Wisnom MR. Demonstration of pseudo-ductility in high performance glass/epoxy composites by hybridisation with thin-ply carbon prepreg. Compos Part A Appl Sci Manuf

2013;52:23–30.
[3] Fuller JD, Jalalvand M, Wisnom MR. Combining fibre rotation and fragmentation to achieve pseudo-ductile CFRP laminates. Compos Struct 2015;142:155–66.
[4] Jalalvand M, Czél G, Wisnom MR. Damage analysis of pseudo-ductile thin-ply UD hybrid composites - a new analytical method. Compos Part A Appl Sci Manuf 2014;69:83–93.
[5] Berbinau P, Soutis C, Goutas P, Curtis PT. Effect of off-axis ply orientation on 0-fibre microbuckling. Compos Part A Appl Sci Manuf 1999;30:1197–207.
[6] Lee J, Soutis C. Measuring the notched compressive strength of composite laminates: Specimen size effects. Compos Sci Technol 2008;68:2359–66.
[7] Arteiro a., Catalanotti G, Xavier J, Camanho PP. Notched response of non-crimp fabric thin-ply laminates. Compos Sci Technol 2013;79:97–114.
[8] Amacher R, Cugnoni J, Botsis J, Sorensen L, Smith W, Dransfeld C. Thin ply composites: Experimental characterization and modeling of size-effects. Compos Sci Technol 2014;101:121–32.
[9] Specimens P. Compressive Properties of Rigid Plastics 1. Annu B ASTM Stand 2008;i:1–8.
[10] ASTM International. D3410M - Standard Test Method for Compressive Properties of Polymer Matrix Composite Materials with Unsupported Gage Section by Shear Loading. Annu B ASTM Stand 2003;15.03:1–16.
[11] ASTM D5467. Standard Test Method for Compressive Properties of Unidirectional Polymer Matrix Composite Materials Using a Sandwich Beam. ASTM Stand 2010;97:1–9.
[12] Fiber C. HexTow ® IMA IM7 Datasheet 2016;000:1–2.
[13] EuroComposites. Mechanical Properties ECA Honeycomb 2010:1.
[14] Bitzer T. Honeycomb Technology Materials, Design, Manufacturing, Applications and Testing. Springer Netherlands; 1997.
[15] Atures E, Ations P. Fm 73 epoxy film adhesive n.d.:1–10.
[16] Yokozeki T, Ogasawara T, Ishikawa T. Nonlinear behavior and compressive strength of unidirectional and multidirectional carbon fiber composite laminates. Compos Part A Appl Sci Manuf 2006;37:2069–79.
[17] Jelf PM, Fleck NA. Compression Failure Mechanisms in Unidirectional Composites. J Compos Mater 1992;26:2706–26.
[18] Properties TF. PYROFIL ™ MR60H 24K 2008.